

## A Study on the Deformation Analysis of Largely Deformed Elasto-Plastic Material Using a Meshfree Method

Kyu-Taek Han<sup>†</sup>

(원고접수일 : 2003년 1월 2일, 심사완료일 : 2003년 3월 12일)

### 무요소법에 의한 대변형 탄소성 재료의 변형해석에 관한 연구

한 기 태\*

**Key words** : meshfree method, RKPM, large deformation, sheet metal, spring back

#### Abstract

Meshfree approximations exhibit significant potential to solve partial differential equations. Meshfree methods have been successfully applied to various problems which the traditional finite element methods have difficulties to handle, including the quasi-static and dynamic fracture, large deformation problems, contact problems, and strain localization problems. Reproducing Kernel Particle Method(RKPM) is used in this research due to its built-in feature of multi-resolution, the sound mathematical foundation and good numerical performance. A formulation of RKPM is reviewed and numerical examples are given to verify the accuracy of the proposed meshfree method for largely deformed elasto-plastic material.

#### 1. 서 론

Despite its success in the analysis of geometrically and materially nonlinear response, the most widely used finite element methods(FEM) in engineering and science are not suitable for problems such as large deformation, high gradients, strain concentration, grain boundary migration, crack propagation and problems associated with frequently remeshing. These reasons are partially

due to the regularity requirement of meshes. Furthermore, mesh generation is a very difficult and lack of robust and efficient 3D mesh generators makes the solution of 3D problems a time-consuming task. To avoid these drawbacks of FEM, so called meshfree(or meshless) methods have been developed during the past 10 years and in recent years, there has been a growing interest in meshfree methods.

A number of meshfree methods have been

<sup>†</sup> 책임저자(부경대학교 기계공학부) E-mail:kthan@pknu.ac.kr, T:051)620-1535

developed to deal with these problems successfully by constructing the approximation functions entirely in terms of particles. The essential feature of these meshfree methods is that the discrete model is completely described by particles. Other noticeable characteristics of the methods are the smooth approximation, ease of adaptability, robustness to large deformations, and robustness to irregularity of particle distributions. Among the meshfree methods, reproducing kernel particle methods(RKPM)[6-14] appears prominent for its sound mathematical foundation and high accuracy. RKPM has been applied with success in various fields such as fluid dynamics[6], large deformation hyper-elastic, and elasto-plastic problems.[9,11-16]

As like many other meshfree methods, RKPM performs domain integration based on Gauss integration for desired accuracy. This integration method requires domain partitioning that is made independently to the nodal discretization. At each Gauss quadrature point, all the nodes with their kernel supports covering that particular Gauss quadrature point are searched, and the stiffness matrix and force vector of this group of influenced nodes need to be computed and assembled. Therefore, the support size of the kernel function and shape function play a significant role in the accuracy and efficiency of RKPM. The supports of the meshfree shape functions usually cover more surrounding points than those in the finite element methods. This requirement increases the number of numerical operations in the stiffness matrix and force vector formations, and the resulting global stiffness matrix has large bandwidth.

The situation is more significant when dealing with incompressible problems, in which sufficiently large support sizes need to be used in the meshfree shape functions to avoid incompressible locking [4,5,9,11-14].

In a meshfree formulation, high-order weight

and kernel functions such as the exponential function, Gaussian function, and the cubic B-spline function are usually used. Therefore, a higher-order Gauss integration is required. An integration order of  $(\sqrt{n+2}) \times (\sqrt{n+2})$ , with  $n$  being the number of points within the integration zone, has been used by Belytschko et al.[5,6] in two-dimensional problems that use an exponential-type weight function. For a two-dimensional integration zone that contains four points, for example, the meshfree methods require  $4 \times 4$  quadrature points, whereas only  $2 \times 2$  quadrature points are needed in 4-node finite elements.

In this paper, we employ RK approximation to formulate the discrete nonlinear equilibrium equations, and frictional contact conditions. The basic theory of RKPM is reviewed in section 2 and we present the application of RKPM to the metal forming problems for largely deformed elasto-plastic material.

## 2. Meshfree Methods

Several different meshfree methods have been developed, including smooth particle hydrodynamics (SPH), element free Galerkin methods(EFG), and reproducing kernel particle methods(RKPM). The earliest development of meshfree methods was the SPH by Lucy[1], and Monaghan[2] for astrophysics problems involving fluid masses arbitrarily moving in an infinite domain. One fundamental feature of SPH is the kernel estimate of the function, where the kernel function can be chosen so that it mimics the Dirac delta function. The method was later extended to treat finite domain problems, however, although the method works well in the absence of boundaries[2] and with a large number of particles, large errors were generated near the boundaries due to the tensile instability and the lack of zero-th order inconsistency as identified by

subsequent researches[4,5,8].

Each of the governing partial differential equations is multiplied by a kernel function and integrated over the solution domain to produce the equations for the kernel estimates. The kernel estimate then provides the approximation to estimate field variables at discrete points. The functions are evaluated only at discrete particles without reference to a finite element mesh.

EFG also enforces the essential boundary conditions by the Lagrange multiplier method. The numerical studies reported in [4,5] suggest that EFG does not exhibit volumetric locking when large supports were used, and the rate of convergence for the method is significantly higher than that of finite elements.

The studies also demonstrated that EFG is very effective in fracture problems that are difficult to handle using finite elements. The efficiency of EFG was later improved with a modified variational principle to enforce essential boundary conditions.

RKPM were proposed by Liu et al.[6-10] to improve the accuracy of the SPH method for finite domain problems.

In this method, the kernel function was modified by introducing a correction function to meet the consistency condition. The resulting reproducing equation with modified kernel function exactly reproduces polynomials to a specific order. It was proven later that the shape functions in RKPM become moving least-squares kernel interpolants if polynomial basis functions are used.

This method provides a general formulation for the construction of shape functions for meshfree computation. The convergence property of RKPM is discussed[8].

Liu et al.[7] introduced wavelets as the kernel functions and successfully applied RKPM to multiscale analysis. Chen et al.[9] introduced a material kernel function for large deformation

analysis so that the kernel stability can be ensured throughout the process of structural deformation. This development also leads to a simplified transformation method on which the transformation matrix and its inversion can be formed at a preprocessing stage. Chen et al.[12-16] later proposed a transformation method with which a modified shape function that possess Kronecker delta properties can be developed to impose essential boundary condition.

## 2.1 Reproducing Kernel Particle Method

### 2.1.1 Construction of One-Dimensional RKPM Basic Function

Consider the following kernel estimate of a function  $u(x)$ :

$$u^*(x) = \int_{-\infty}^{\infty} \Phi_a(x-s)u(s) ds \quad (2.1)$$

where  $u^*(x)$  is the kernel estimate of  $u(x)$ , and  $\Phi_a(x-s)$  is the kernel function with the support measure of 'a'. In general,  $a$  is defined so that it determines the domain of influence  $\Phi_a(x)$  to the neighborhood of  $s=x$ .

If the kernel function is a Dirac delta function, the  $u^*(x)$  exactly generates  $u(x)$ . In practice, however, the domain is finite in structural problems, and the Dirac delta function is difficult to deal with numerically. Therefore, for a bounded domain, Eq.(2.1) is rewritten by

$$u^*(x) = \int_{\Omega} \Phi_a(x-s)u(s) ds \quad (2.2)$$

where  $\Phi_a(x-s)$  is a positive function with the following properties:

$$\int_{\Omega} \Phi_a(x-s) ds = 1 \quad (2.3)$$

$$u^x(x) \rightarrow u(x) \text{ as } a \rightarrow 0 \quad (2.4)$$

In fact, a zero-th consistency condition(Eq.(2.3)) can be easily satisfied by the normalization of the kernel function. However, when the domain of interest is finite, Eq.(2.3) does not assure the consistency condition in the discrete form. To study this problem, Liu et al.[6] investigated the reproductivity of kernel estimate using a Taylor series expansion of the function  $u(s)$  around  $x$ . Consider here a one-dimensional kernel estimate for simplicity, and let

$$u(s) = \sum_{n=0}^{\infty} \frac{(s-x)^n}{n!} u^{(n)}(x) \quad (2.5)$$

$$\text{where } u^{(n)} \equiv \frac{d^n u}{d x^n}.$$

Substituting Eq.(2.5) into Eq.(2.2) leads to

$$u^x(x) = m_0(x)u(x) + \sum_{n=1}^{\infty} \frac{(-1)^n}{n!} m_n(x) u^n(x) \quad (2.6)$$

where  $m_n(x)$  is the moment defined by

$$m_n(x) = \int_{\Omega_x} (x-s)^n \Phi_a(x-s) ds \quad (2.7)$$

To preserve the N-th order consistency condition in  $u^x(x)$ , the kernel function has to satisfy the so-called reproducing conditions[6]:

$$m_0(x) = 1; \quad m_\kappa(x) = 0 \text{ for } 1 \leq \kappa \leq N \quad (2.8)$$

However, the higher-order consistency conditions are difficult to meet, and most of the kernel functions do not satisfy these reproducing conditions.

Liu et al.[6] introduces a correction function to the kernel estimate:

$$u^R(x) = \int_{\Omega_x} C(x; x-s) \Phi_a(x-s) u(s) ds \quad (2.9)$$

where  $u^R(x)$  is the "reproduced" function of  $u(x)$ ,  $C(x; x-s)$  is called the correction function that is to be constructed to fulfill reproducing conditions, and Eq.(2.9) is the reproducing kernel approximation, or the reproducing equation.

The correct function is expressed by an Nth order polynomial of  $(x-s)$ , i.e.

$$C(x; x-s) = \sum_{i=0}^N b_i(x)(x-s)^i \quad (2.10) \\ \equiv b^T(x)H(x-s)$$

where  $H(x-s)$  is the vector of polynomial basis functions,

$$H^T(x-s) = [ 1, x-s, (x-s)^2, \dots, (x-s)^N ] \quad (2.11)$$

$$b^T(x) = [ b_0(x), b_1(x), b_2(x), \dots, b_N(x) ]$$

and  $b_i(x)$ 's are determined by satisfying the reproducing conditions, i.e.,

$$\int_{\Omega} C(x; x-s) \Phi_a(x-s) H(x-s) ds \\ = H(0) \quad (2.12)$$

Substituting Eq.(2.10) into Eq.(2.12) leads to

$$[ \int_{\Omega} H(x-s) \Phi_a(x-s) H^T(x-s) ds ] b(x) \\ = H(0) \quad (2.13)$$

and the unknown vector  $b(x)$  is solved by

$$b(x) = M(x)^{-1} H(0) \quad (2.14)$$

$$M(x) = \int_{\Omega} H(x-s) H^T(x-s) \Phi_a(x-s) ds \quad (2.15)$$

Introducing Eqs.(2.10) and (2.14) into Eq.(2.9) results in the following reproducing kernel approximation:

$$\begin{aligned} u^R(x) &= \int_{\Omega_x} C(x; x-s) \Phi_a(x-s) u(s) ds \\ &= H^T(0) M^{-1}(x) \\ &\quad \times \int_{\Omega} H(x-s) \Phi_a(x-s) u(s) ds \end{aligned} \quad (2.16)$$

Eq.(2.16) can be rewritten in the following form,

$$u^R(x) = \int_{\Omega_x} \Phi_a(x; x-s) u(s) ds \quad (2.17)$$

where

$\Phi_a(x; x-s) = C(x; x-s) \Phi_a(x-s)$  is called the reproduced kernel. Since Eq.(2.17) exactly reproduces N-th order polynomials, the method fulfills the N-th order consistency conditions, i.e.,

$$\begin{aligned} \int_{\Omega_x} \Phi_a(x; x-s) s^n ds &= x^n \\ \text{for } n &= 0, \dots, N \end{aligned} \quad (2.18)$$

### 2.1.2 Discretization of Reproducing Kernel

#### Approximation

The discretized reproducing equation is obtained by performing numerical integration in Eq.(2.17). Suppose that the domain  $\Omega_x$  is discretized by a set of nodes  $\{x_1, \dots, x_{NP}\}$ , where  $x_I$  is the location of node I, and NP is the total number of points(nodes). By the use of a simple trapezoidal rule, Eq.(2.17) is discretized into

$$u^h(x) = \sum_{I=1}^{NP} \Psi_I^a(x) d_I \quad (2.19)$$

$$\text{where } \Psi_I^a(x) = \Phi_a(x; x-x_I) \Delta x_I \quad (2.20)$$

The function  $\Psi_I^a(x)$  is interpreted as the particle or meshfree shape function of node I, and  $d_I$  is the associated coefficient of approximation. Note this shape function does not meet the Kronecker delta properties, i.e.,  $\Psi_I^a(x_J) \neq \delta_{IJ}$ , which means generally  $u^h(x) \neq d_I$  and  $d_I$  is not the nodal value of the function computed at the particle I. This leads to some complication in imposing the essential boundary conditions in the meshfree method. Additional development such as the Lagrange multiplier method[4] or the transformation method[9] is required to impose the essential boundary conditions. A singular kernel method was also proposed for direct imposition of essential boundary conditions, but the solution accuracy of linear basis functions was poor.

The discrete reproducing conditions are preserved if the numerical integration of  $M$  and  $M^{-1}$  is consistent with the discretization of the reproducing equation. Since the discretization of the continuous reproducing equation is to obtain the shape functions, the weight of the discretization  $\Delta x_I$  in Eq.(2.20) is set to unity for simplicity. It can be shown that the Reproducing Kernel shape function meets the following consistency conditions:

$$\sum_{I=1}^{NP} \Psi_I^a(x) x_I^n = x^n; \quad n = 0, N \quad (2.21)$$

Widely used kernel functions include exponential function[4], Gaussian function, and cubic B-spline function, among others. In this study, the cubic B-spline function is used as the kernel function:

$$\begin{aligned} & 2/3 - 4|z|^2 + 4|z|^3 \\ & \text{for } 0 \leq |z| \leq \frac{1}{2} \\ \Phi_a(z) & 4/3 - 4|z| + 4|z|^2 - 4/3|z|^3 \\ & \text{for } \frac{1}{2} \leq |z| \leq 1 \\ & 0 \\ & \text{otherwise} \end{aligned}$$

where  $z = \frac{x - x_l}{a}$

### 3. Meshfree Formulation in Elasto-plastic Material with Contact Conditions

Contact conditions are included to handle contact between tools and workpiece. The classical Coulomb law is used to model frictional contact and the penalty method is applied to assure impenetration. The contact traction's  $t_n$  and  $t_t$  in the normal and tangential directions, respectively, are defined as follows:

$$t_n = -\alpha_n g_n \quad (2.31)$$

$$t_t = \begin{cases} -\alpha_t g_t & \text{if } \left| \alpha_t g_t \right| \leq \left| \mu_t t_n \right| \\ & \text{(stick conditions)} \\ -\mu_t t_n \operatorname{sgn}(g_t) & \text{otherwise} \\ & \text{(slip conditions)} \end{cases} \quad (2.32)$$

where  $\mu$  is the coefficient of friction,  $\alpha_n$  and  $\alpha_t$  are the normal and tangential penalty numbers, and  $g_n$  and  $g_t$  are normal and tangential gaps between contact surfaces. The variational equation of the problem can be written as:

$$\begin{aligned} & \int_{\Omega_x} \delta u_{i,j} \tau_{i,j} d\Omega \\ & - \int_{\Omega_x} \delta u_i b_i d\Omega - \int_{\Gamma_x^{h_i}} \delta u_i h_i d\Gamma \\ & + \int_{\Gamma_x^c} (t_n \delta g_n + t_t \delta g_t) d\Gamma = 0 \end{aligned} \quad (2.33)$$

The contact term is integrated by collocation formulation to yield

$$\begin{aligned} & \int_{\Gamma_x^c} (t_n \delta g_n + t_t \delta g_t) d\Gamma \\ & = \sum_A (F_n \delta g_n + F_t \delta g_t)_A \end{aligned} \quad (2.34)$$

where  $\Omega_x$  is the domain,  $\Gamma_x^{h_i}$  is the current non-contact traction boundary,  $\Gamma_x^c$  is the contact boundary,  $\tau_{i,j}$  is the Cauchy stress,  $b_i$  is the body force,  $h_i$  is the non-contact surface traction,  $F_n$  and  $F_t$  are the nodal normal and tangential contact forces and  $A$  is summed over the contact nodes on the deformable body.

The reproducing kernel shape functions as described in Eq.(2.20) and (2.29) are used in a Galerkin approximation of the variational equation, Eq.(2.33). The coordinate transformation method[9] is used in the discrete RKPM equation so that the contact force  $F_n$  and  $F_t$  are nodal quantities. The linearization of Eq.(2.33) leads to a tangential stiffness, and the explicit expression of contact stiffness and contact force in RKPM framework can be found in [12].

The radial return mapping algorithm is used to compute the stress and internal variables and the consistent tangent operator, which preserves the quadratic convergence rate of the Newton method, is used. The matrix equations and numerical procedures are given in detail in[9].

## 4. Numerical Examples

### 4.1 Sheet Metal Forming by a Cylindrical Punch

The numerical results from the RKPM are compared with the analytical solutions. A plane-strain sheet metal is stretched by a

cylindrical punch as shown in Fig.1. This problem is recommended as a benchmark test of sheet metal forming processes. In this problem, the sheet metal forming process is considered to be quasi-static, and punch and die are assumed to be perfectly rigid. The dimension of the problem are  $R_p=50.8\text{mm}$ ,  $C_d=59.18\text{mm}$ ,  $R_0=61.30\text{mm}$ ,  $R_d=6.35\text{mm}$ , and  $h=1.0\text{mm}$ . The constitutive law of sheet metal is described using a  $J_2$  plasticity with material constants : Young's modulus  $E=69\text{GPa}$ , Poisson's ratio  $\nu=0.3$ , isotropic hardening  $\sigma_y(\epsilon^p)=589(10^{-4} + \epsilon^p)^{0.216}$  MPa, and coefficient of friction  $\mu=0$ . Due to symmetry, only half of the sheet metal is modeled with  $4 \times 51$  particles and  $3 \times 50$  integration zones, and Gauss integration order of  $4 \times 4$  is used. Relatively dense particles are distributed around the die corners in order to capture stress concentrations in those areas. In this analysis, the end of the sheet metal is fixed, and the rigid punch is moved downward with a vertical displacement of  $30\text{mm}$  in 50 incremental steps. Reproducing kernel contact formulation and kinematic constraints treatments[15] are employed for the contact analysis.

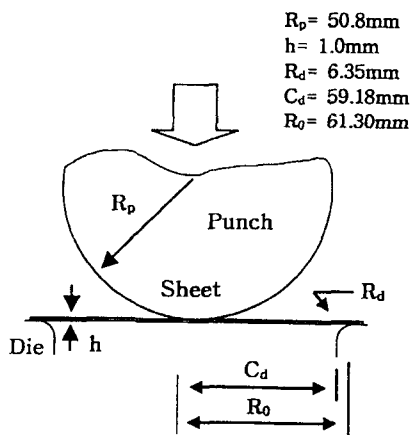


Fig. 1 Geometry of plain-strain cylindrical punch problem.

The RKPM prediction is compared with the membrane analytical solution[3] in Fig.3. The results show that RKPM solution agrees well with the membrane solution. Note that the membrane solution does not take necking deformation into consideration. The progressive deformation of the sheet metal is shown in Fig.2, and local necking are observed near the die contact areas. In this analysis, the tolerance for the residual force norm is  $10^{-6}$ .

#### 4.2 Springback of a Sheet Metal in Flanging

A straight flanging operation and its springback behavior of a sheet metal is simulated, and the predicted springback angle is compared with experimental data reported in Song et al[17]. The blank is  $150\text{mm}$  in length,  $150\text{mm}$  in width and  $1\text{mm}$  in thickness. The design parameters of a flanging operation are shown in Fig.4, where the flange length  $L=20\text{mm}$ , die radius  $R=3\text{mm}$ , and

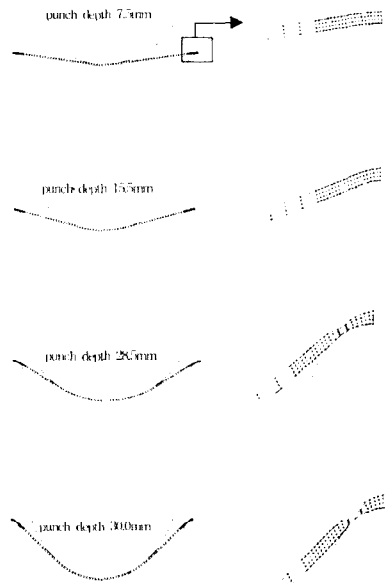
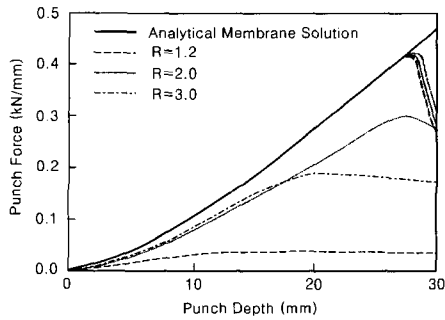
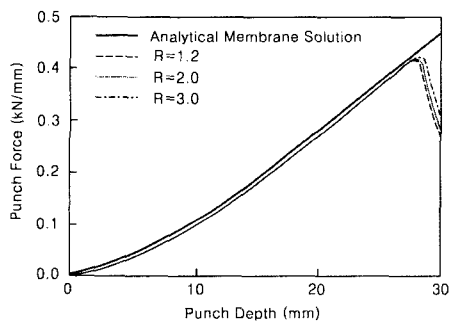


Fig. 2 Progressive deformation of a cylindrical punch.

three different gaps,  $G=1.2, 1.6,$  and  $2.0\text{mm}$  are considered in this analysis. The material properties are Young's modulus  $E=70\text{GPa}$ , Poisson's ratio  $\nu=0.3$ , isotropic hardening  $\sigma_y(\epsilon^p) = 146 + 500\epsilon^p$  MPa.



(a) Direct nodal integration



(b) SC nodal integration

**Fig. 3 Comparison of the cylindrical punch force-displacement response.**

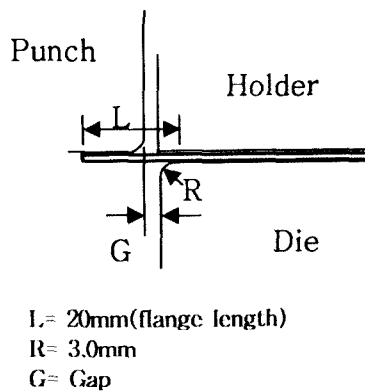


**Fig. 4 Geometry parameters of flanging problem and description.**

The predicted angles of springback for three gap dimensions  $G=1.2, 1.6,$  and  $2.0$  are compared with experimental data[17] as shown in Fig.5. In meshfree discretization,  $3 \times 101, 4 \times 116,$  and  $5 \times 131$  nodes with three shape function support sizes  $r=1.2, 2.0,$  and  $3.0$  are used and compared. The meshfree results show good agreement with experimental data, where the springback angle increases as the gap dimension increases. The results also demonstrate that the meshfree discretization with larger shape function support size provides a better agreement with the experimental data. Typical flanging progressive deformations using  $5 \times 131$  nodes and shape function normalized support size of  $2.0$  are shown in Fig.6. The comparison of deformation and springback under different gap dimensions are displayed in Fig.7.

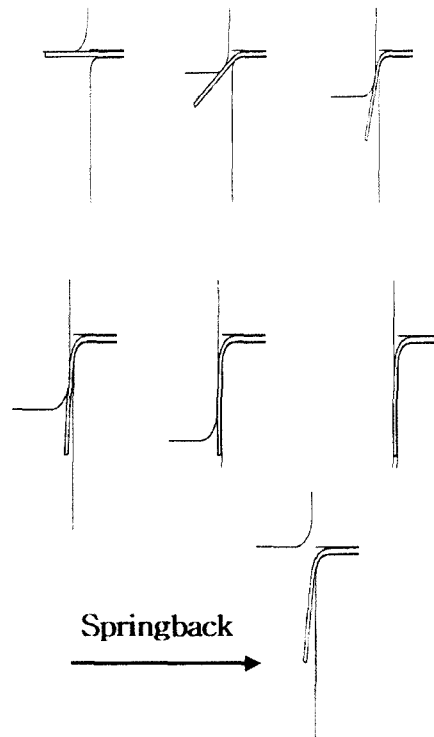


**Fig. 6 Deformation and springback of the flanging operation simulated by meshfree method.**



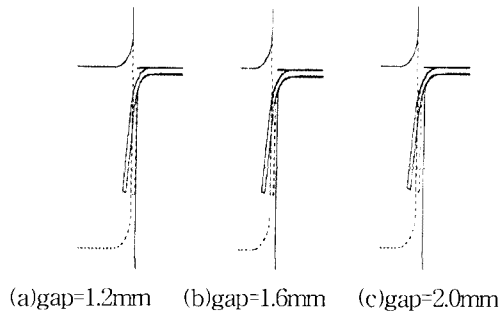


Fig. 7 Effect of gap dimension on springback.

### 5. Conclusions

A meshfree formulation for loading history-dependent material behavior and frictional contact conditions is developed based on the Reproducing Kernel Producing Method(RKPM) for the metal forming simulation. The emphasis is on the meshfree treatment of large plastic deformation and complicated contact conditions. The numerical examples show that no mesh distortion difficulties in the finite element analysis are encountered by usage of a smooth kernel function with flexibly adjustable support size.

Due to the use of the Lagrangian reproducing kernel shape functions, the support size of the kernel functions does not require readjustment during the contact computation and the large plastic deformation induced in the metal forming process can be dealt with easily by the proposed method.

### Acknowledgement

The author gratefully acknowledges the financial support of the Pukyong National University under the Pukyong Research Abroad Program in 2001.

This paper was partially supported by the Brain Korea 21 Project in 2003.

### References

- [1] L.Lucy,"A Numerical Approach to the Testing of the Fission Hypothesis", *Astronomical Journal*, 82, 1013-1024, 1977
- [2] J.J.Monaghan,"An Introduction to SPH", *Computer Physics Communications*,48, 89-96, 1988
- [3] S.Choudhry and J.K.Lee, "Dynamic Plain-Strain Element Simulation of Industrial Sheet-Metal Forming Processes", *International Journal of Mechanical Sciences*, 36, 189-207, 1994
- [4] T.Belytschko, Y.Y.Lu, and L.Gu, "Element-Free Galerkin Methods", *International Journal for Numerical Methods in* 229 256, 1994
- [5] Y.Y.Lu, T.Belytschko, and L.Gu, "A New Implementation of the Element Free Galerkin Method", *Computer Methods in Applied Mechanics and Engineering*,113, 397-414, 1994
- [6] W.K.Liu, S.Jun, and Y.F.Zhang, "Reproducing Kernel Particle Methods", *International Journal for Numerical Methods in Fluids*, 20, 1081-1106, 1995
- [7] W.K.Liu and Y.J.Chen, "Wavelet and Multiple Scale Reproducing Kernel Particle Methods", *International Journal for Numerical Methods in Fluids*, 21, 901-931, 1995
- [8] W.K.Liu, Y.Chen, C.T.Chang, and T. Belytschko, "Advanced in Multiple Scale Kernel Particle Methods", *Computational Mechanics*, 18, 73-111, 1996
- [9] J.S.Chen, C.Pan, C.T.Wu, and W.K.Liu, "Reproducing Kernel Particle Methods for Large Deformation Analysis of Nonlinear Structures", *Computer Methods in Applied Mechanics and Engineering*, 139, 195-227, 1996
- [10] W.K.Liu, W.Hao, Y.Chen, et al, "Multiresolution Reproducing Kernel Particle Methods", *Computational Mechanics*, 20, 295-309, 1997

- [11] J.S.Chen, C.Pan, C.Roque, and H.P. Wang, "A Lagrangian Reproducing Kernel Particle Method for Metal Forming Analysis", *Computational Mechanics*, 22, 289-307, 1998
- [12] J.S.Chen, C.T.Wu, and C.Pan, "Application of Reproducing Kernel Particle Methods to Large Deformation and Contact Analysis of Elastomers", *Rubber Chemistry and Technology*, 71, 191-213, 1998
- [13] J.S.Chen, C.Roque, C.Pan, and S.T. Button, "Analysis of Metal Forming Process Based on Meshless Method", *Journal of Materials Processing Technology*, 80, 642-646, 1998
- [14] J.S.Chen, S.Yoon, H.P.Wang, and W.K. Liu, "An Improved Reproducing Kernel Particle Method for Nearly Incompressible Finite Elasticity", *Computer Methods in Applied Mechanics and Engineering*, 181, 117-146, 2000
- [15] J.S.Chen and H.P.Wang, "New Boundary Condition Treatments for Meshless Computation of Contact Problems", *Computer Methods in Applied Mechanics and Engineering*, 187, 441-468, 2000
- [16] N.H.Kim, K.K.Choi, and J.S.Chen, "Die Shape Design Optimization of Sheet Metal Stamping Process Using Meshfree Method", *International Journal for Numerical Methods in Engineering*, 51, 1385-1405, 2001
- [17] N.Song, D.Qian, J.Cao, W.K.Liu, and S.Li, "Effective Models for Prediction of Springback in Flanging", accepted *ASME Journal of Engineering Materials and Technology*, 2001

## 저 자 소 개



### 한규택 (韓圭澤)

1958년 10월생, 1982년 부산대학교 기계공학과 졸업. 1984년 부산대학교 대학원 기계공학과 졸업(석사). 1988년 부산대학교 대학원 기계공학과 졸업(박사). 2001년 미국 The University of Iowa 교환교수. 1998년 9월 ~ 현재 부경대학교 기계공학부 교수